Supplement of Atmos. Chem. Phys., 22, 15603–15620, 2022
https://doi.org/10.5194/acp-22-15603-2022-supplement

Supplement of

Emission factors and evolution of SO_2 measured from biomass burning in wildfires and agricultural fires

Pamela S. Rickly et al.

Correspondence to: Pamela S. Rickly (pamela.rickly@state.co.us) and Andrew W. Rollins (andrew.rollins@noaa.gov)

Section 1: Sulfur modeling

In the absence of photochemical reactions due to reduced infiltration of sunlight, sulfate aerosols are expected to be produced through aqueous reactions with existing particles or cloud droplets. This requires the dissolution of SO_2 onto existing particles to produce S(IV) ($= SO_2 \cdot H_2O_{(aq)} + HSO_3^- + SO_3^{2-}$) compounds in equilibria. However, the pathway of S(IV) oxidation is highly dependent on the pH and ionic strength of the existing particles as well as the available liquid water content (LWC) (Zhang et al., 2015; Shao et al., 2019). Under more acidic conditions (pH<5), S(IV) oxidation occurs primarily through reaction with H_2O_2. At higher pH values, oxidation by dissolved O_3 and NO_2 begin to dominate (Guo et al., 2017). As a result, modeling of such events is highly dependent on the aerosol pH.

Direct measurements of aerosol pH are not available for this study. As a result, several methods have been suggested for calculating aerosol acidity, including ion balance, molar ratio, and thermodynamic models. Ion balance and molar ratio estimates can be used to assess the proton loading of the air mass by comparing the number of cations present to anions (Hennigan et al. (2015). However, Hennigan et al. (2015) and Guo et al. (2015) discourage the use of these methods because they disregard acidic and ionic partial dissolution and the effects of the aerosol LWC on pH calculations, which is of concern in moderately acidic to alkaline environments such as fires (Pye et al., 2020). Thermodynamic models more accurately predict the partitioning of $NH_{4(p)}$-$NH_{3(g)}$ and $NO_{3(p)}$-$HNO_{3(g)}$ for inferring the hydronium ion concentration and pH compared to the other methods while also predicting LWC (Hennigan et al., 2015). These models require the known chemical component inputs of both the gas and aerosol concentrations measured within the air mass as inputs, along with temperature and relative humidity to calculate the hydronium ion concentration (Hennigan et al., 2015; Guo et al., 2015; Ding et al., 2019). Yet, even with the inclusion of thermodynamic calculations of pH and LWC, model predictions of sulfate aerosol production in Beijing during heavy pollution events were underestimated by 65% (Shao et al., 2019). As a result, additional pathways of S(IV) oxidation have been proposed, including oxidation by NO_2 and O_2 through catalytic reactions involving transition metal ions (Moch et al., 2018; Cheng et al., 2016; Shao et al., 2019).

Dovrou et al. (2019) observed that hydroxymethanesulfonate (HMS) can be misidentified as inorganic sulfate in ion chromatography and aerosol mass spectrometry measurements. Using an analytical column composed of an alkyl quaternary ammonium functional group, Dovrou et al. (2019) were able to separate the two species. This suggests that organosulfates or organosulfonates could be the source of the discrepancy between measurements and models in urban areas.

The chemistry of HMS production and reversal has been extensively studied through laboratory measurements (Boyce and Hoffmann, 1984; Deister et al., 1986; Kok et al., 1986) and model simulations (Moch et al., 2018; Song et al., 2019, 2021). A review of these laboratory studies and the parameters for the determination of the rate constants is provided by Song et al. (2021). While the Song et al. (2021) study explored the use of lower HMS formation kinetic rates under cloud conditions, this study finds better agreement with the measurements using the higher rates along with the reverse reaction rate established by Song et al. (2021) (based on Boyce and Hoffmann (1984) and Deister et al. (1986) measurements) under aerosol conditions. While HMS is resistant to reaction with H_2O_2, aqueous phase reaction of HMS with OH radicals is likely to occur (Olson and Fessenden, 1992). However, aqueous OH is short-lived and when included in the model, through condensation and evaporation (Eqs. 3.6 and 3.7 in main paper), produced no change in the model results.

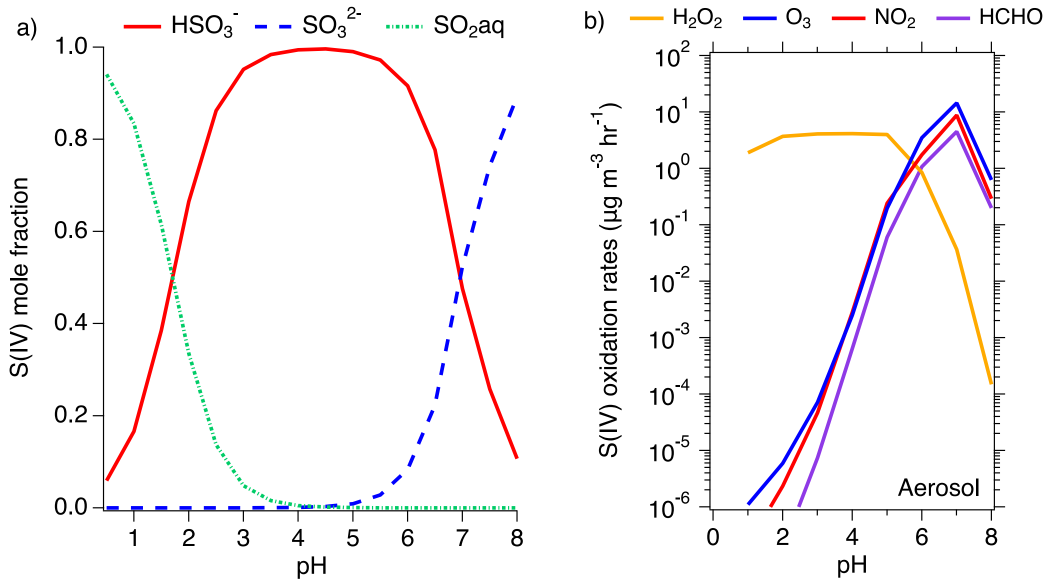

Figure S1. Sulfur conversion based on pH dependence for a) S(IV) production as SO_2 enters the aqueous phase with ideal solution assumption and b) the rate of S(IV) oxidation based on oxidizing species mixing ratios of 3.3 ppb for SO_2, 82 ppb for O_3, 1.6 ppb for H_2O_2, 9 ppb for NO_2, and 29 ppb for HCHO with 200 μg m^{-3} LWC. While H_2O_2, O_3, and NO_2 produce inorganic sulfate, HCHO produces HMS.

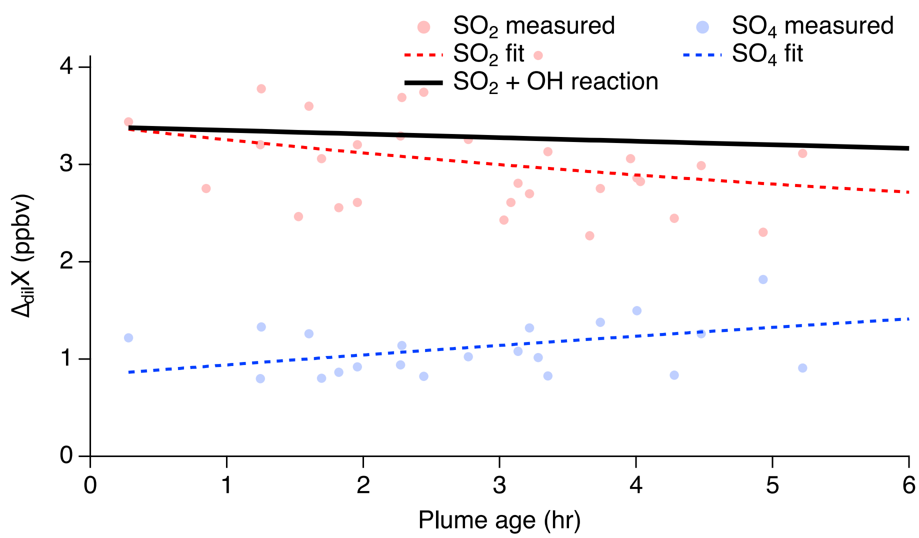

Figure S2. Calculation of the OH contribution to the SO_2 decay observed during the 3 August 2019 FIREX-AQ flight.

Table S1. List of aqueous phase reactions included as the heterogeneous mechanism in the F0AM 0-D model in which the rates of condensation (k_{cond}) and evaporation (k_{evap}) require the particle surface area (S_a), Henry's Law constant (H), liquid water content (LWC), and hydronium ion concentration (H^+, calculated from pH). Rates of HMS reaction with S(IV) used in GEOS-Chem are also listed for comparison.

Reaction	Rate constant ($M^{-1}\ s^{-1}$)	Reference	GEOS-Chem
$SO_2 \rightarrow S(IV)$	$k_{cond} = 0.25 \cdot \gamma \cdot c \cdot S_a$	Seinfeld and Pandis (2006)	
$SO_{2(aq)} \rightarrow SO_{2(g)}$	$k_{evap} = {k_{cond}}/{(H \cdot LWC)}$	D'ambro et al. (2016)	
$HSO_3^- \rightarrow SO_{2(g)}$	$k_{evap} = {(k_{cond} \cdot H^+)}/{(H \cdot LWC \cdot K_1)}$	D'ambro et al. (2016); Seinfeld and Pandis (2006)	
$SO_3^{2-} \rightarrow SO_{2(g)}$	$k_{evap} = {(k_{cond} \cdot (H^+)^2)}/{(H \cdot LWC \cdot K_1 \cdot K_2)}$	D'ambro et al. (2016); Seinfeld and Pandis (2006)	
$O_{3(aq)} + SO_{2(aq)} \rightarrow SO_4^{2-} + HSO_4^-$	$k = 2.4 \times 10^4$	Kreidenweis et al. (2003)	
$O_{3(aq)} + HSO_3^- \rightarrow SO_4^{2-} + H^+ + O_{2(aq)}$	$k = 3.7 \times 10^5 \cdot \exp\left(-5530\left(\frac{1}{T} - \frac{1}{298}\right)\right)$	Hoffmann and Calvert (1985)	
$O_{3(aq)} + SO_3^{2-} \rightarrow SO_4^{2-} + O_{2(aq)}$	$k = 1.5 \times 10^9 \cdot \exp\left(-5280\left(\frac{1}{T} - \frac{1}{298}\right)\right)$	Hoffmann and Calvert (1985)	
$H_2O_{2(aq)} + HSO_3^- \rightarrow SO_4^{2-} + 2H^+ + H_2O$	$k = \frac{7.45 \times 10^7 \cdot H^+ \cdot \exp\left(-4430\left(\frac{1}{T} - \frac{1}{298}\right)\right)}{1 + 13 \cdot H^+}$	Hoffmann and Calvert (1985)	
$2NO_{2(aq)} + HSO_3^- \rightarrow 3H^+ + 2NO_2^- + SO_4^{2-}$	$k = 1 \times 10^6$	Liu and Abbatt (2021)	
$2NO_{2(aq)} + SO_3^{2-} \rightarrow 3H^+ + 2NO_2^- + SO_4^{2-}$	$k = 1.4 \times 10^{10}$	Liu and Abbatt (2021)	
$HCHO \rightarrow HCHO_{(aq)}$	$k_{cond} = 0.25 \cdot \gamma \cdot c \cdot S_a$	Seinfeld and Pandis (2006)	
$HCHO_{(aq)} + HSO_3^- \rightarrow CH_2OHSO_3^-$	$k = 7.9 \times 10^2 \cdot \exp\left(-4900\left(\frac{1}{T} - \frac{1}{298}\right)\right)$	Boyce and Hoffmann (1984)	$k = 7.9 \times 10^2 \cdot \exp\left(-16.435\left(\frac{298}{T} - 1\right)\right)$
$HCHO_{(aq)} + SO_3^{2-} \rightarrow CH_2OHSO_3^-$	$k = 2.5 \times 10^7 \cdot \exp\left(-1800\left(\frac{1}{T} - \frac{1}{298}\right)\right)$	Boyce and Hoffmann (1984)	$k = 2.5 \times 10^7 \cdot \exp\left(-6.037\left(\frac{298}{T} - 1\right)\right)$
$CH_2OHSO_3^- \rightarrow HCHO_{(aq)} + HSO_3^-$	$k = 6.2 \times 10^{-8} \cdot \exp\left(-11400\left(\frac{1}{T} - \frac{1}{298}\right)\right)$	Song et al. (2021)	
$\rightarrow HCHO_{(aq)} + SO_3^{2-}$	$+4.8 \times 10^3 \cdot \left({K_w}/{H^+}\right) \cdot exp\left(-4700\left(\frac{1}{T} - \frac{1}{298}\right)\right)$		

Table S2. Measurements used for model initial concentrations and constraints.

Measurement	Method
Sulfur dioxide (SO_2), nitric oxide	NOAA Laser-Induced Fluorescence (LIF)
Sulfate (SO_4), organosulfur	Aerodyne Aerosol Mass Spectrometry (AMS)
Carbon monoxide	Differential Absorption Carbon monOxide Measurement (DACOM)
Sulfate, sulfite	Soluble Acidic Gases and Aerosols (SAGA)
Formaldehyde	NASA In Situ Formaldehyde (ISAF)
Ozone, nitrogen dioxide	NOAA NOyO3 Chemiluminescence
Hydrogen peroxide	Caltech Chemical Ionization Mass Spectrometry (CIT CIMS)
Aerosol surface area	TSI Laser Aerosol Spectrometer (LAS) 3340
Cloud indicator	Cloud, Aerosol, and Precipitation Spectrometer (CAPS)
Actinic flux	Charged-coupled device Actinic Flux Spectroradiometer (CAFS)
Pressure, altitude, temperature, relative humidity, solar zenith angle	Meteorological and Navigation Facility Instrumentation

Table S3. Mass accommodation (α) and gas diffusion coefficients (Dg) used for deriving the gas-phase diffusion limitations of SO_2, O_3, H_2O_2, NO_2, and HCHO.

Compound	Variable	Formula/Value	Reference
SO_2	α	$1 + \exp(14.7 - {}^{3825}/_{T}))^{-1}$	Boniface et al. (2000)
	Dg	$(\frac{1013 \times 94}{760 \times P} \times \frac{T}{296})^{1.75}$	Tang et al. (2014)
O_3	α	0.47	Vieceli et al. (2005)
	Dg	$\frac{410}{660} \times (\frac{1013 \times 178}{760 \times P} \times \frac{T}{296})^{1.75}$	Tang et al. (2014)
H_2O_2	α	0.23	Seinfeld and Pandis (2016)
	Dg	$(\frac{1013 \times 116}{760 \times P} \times \frac{T}{296})^{1.75}$	Tang et al. (2014)
NO_2	α	0.0015	George et al. (1992)
	Dg	$(\frac{1013 \times 106}{760 \times P} \times \frac{T}{296})^{1.75}$	Tang et al. (2014)

HCHO	α	0.04	Finlayson-Pitts and Pitts (1999)
	Dg	0.152	Toda et al. (2014)

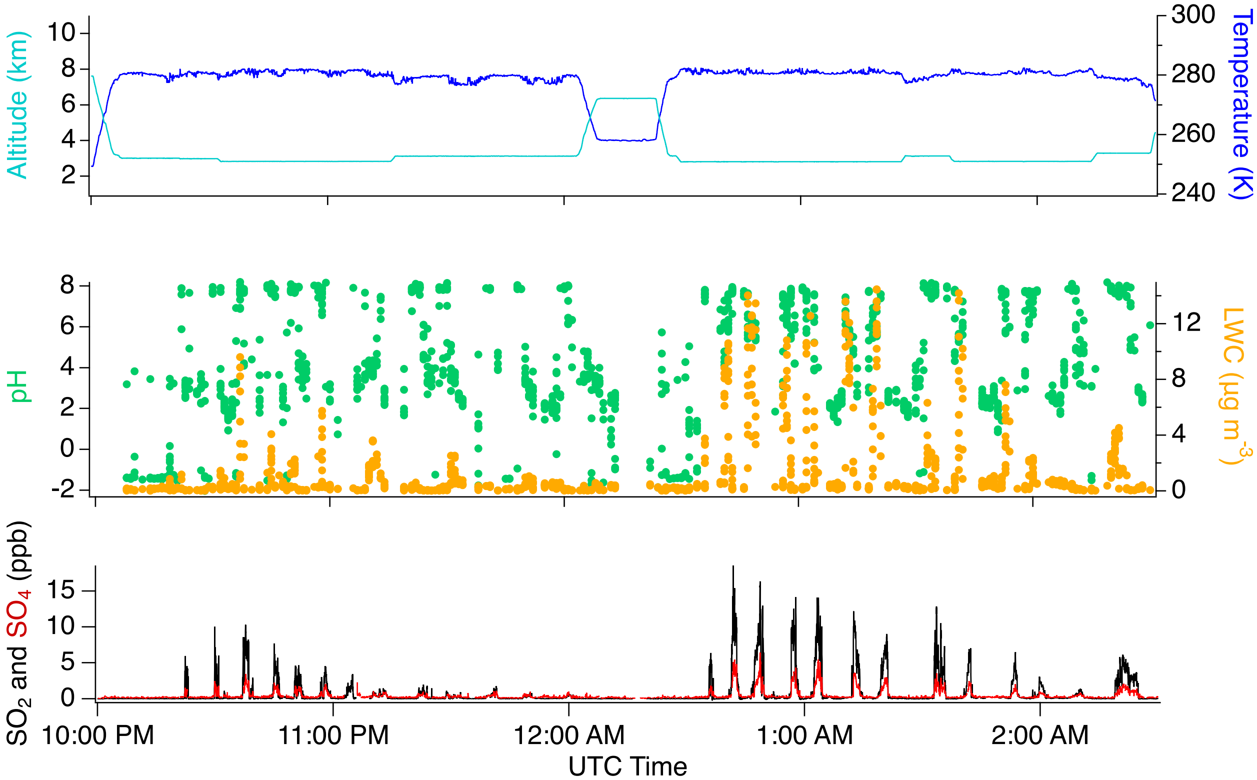

Figure S3. Measurements of SO_2, sulfate, temperature, and altitude with calculations of pH and LWC during the 3 August 2019 flight.

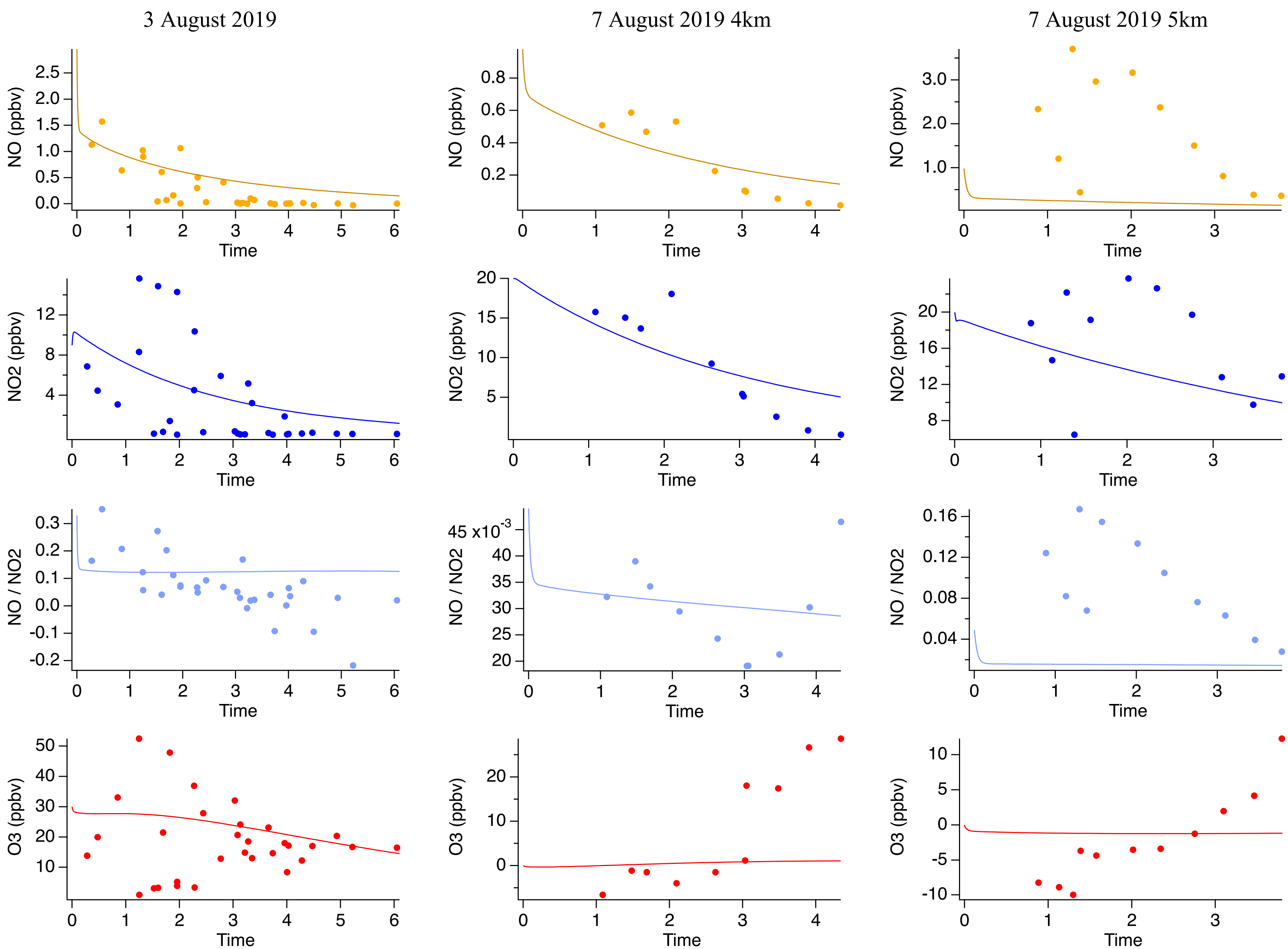
3 August 2019
7 August 2019 4km
7 August 2019 5km
NO (ppbv)
NO2 (ppbv)
NO / NO2
O3 (ppbv)
Time
45 x10^-3

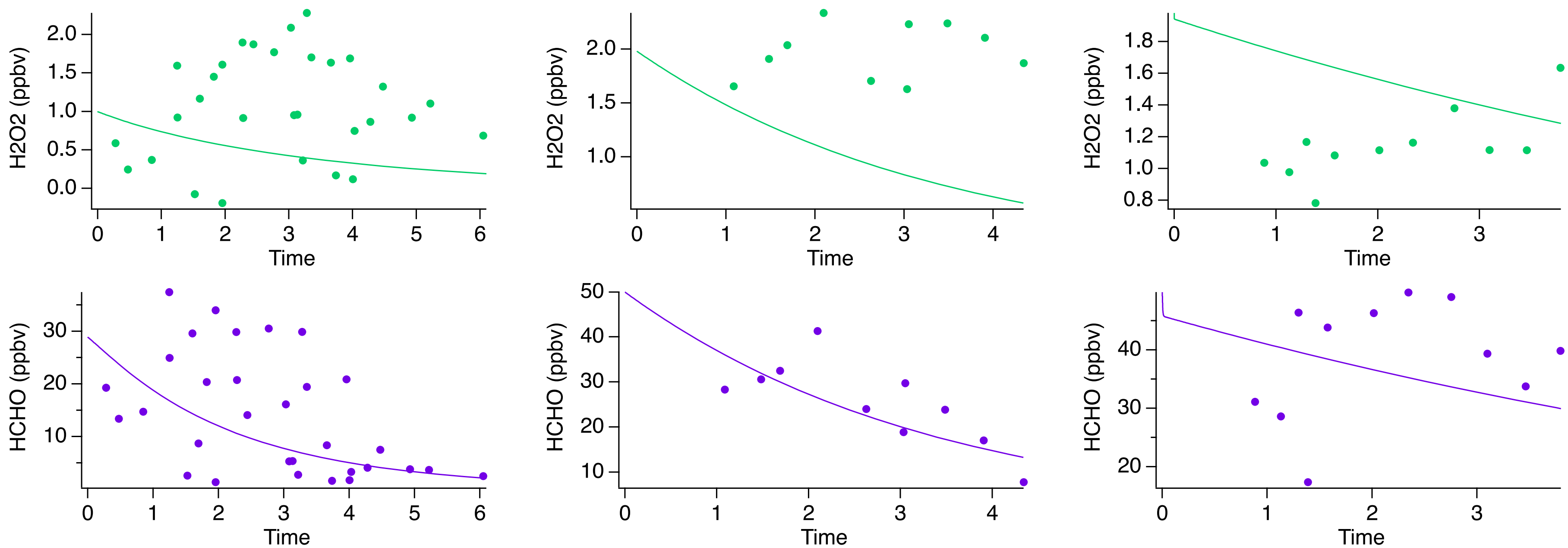

Figure S4. Model results for NO, NO_2, NO/NO_2, O_3, H_2O_2, and HCHO compared to the dilution normalized measurements for each modeled flight. While H_2O_2 shows moderate agreement, it should be noted that organic aerosol may be a source of H_2O_2 (Ye et al., 2021).

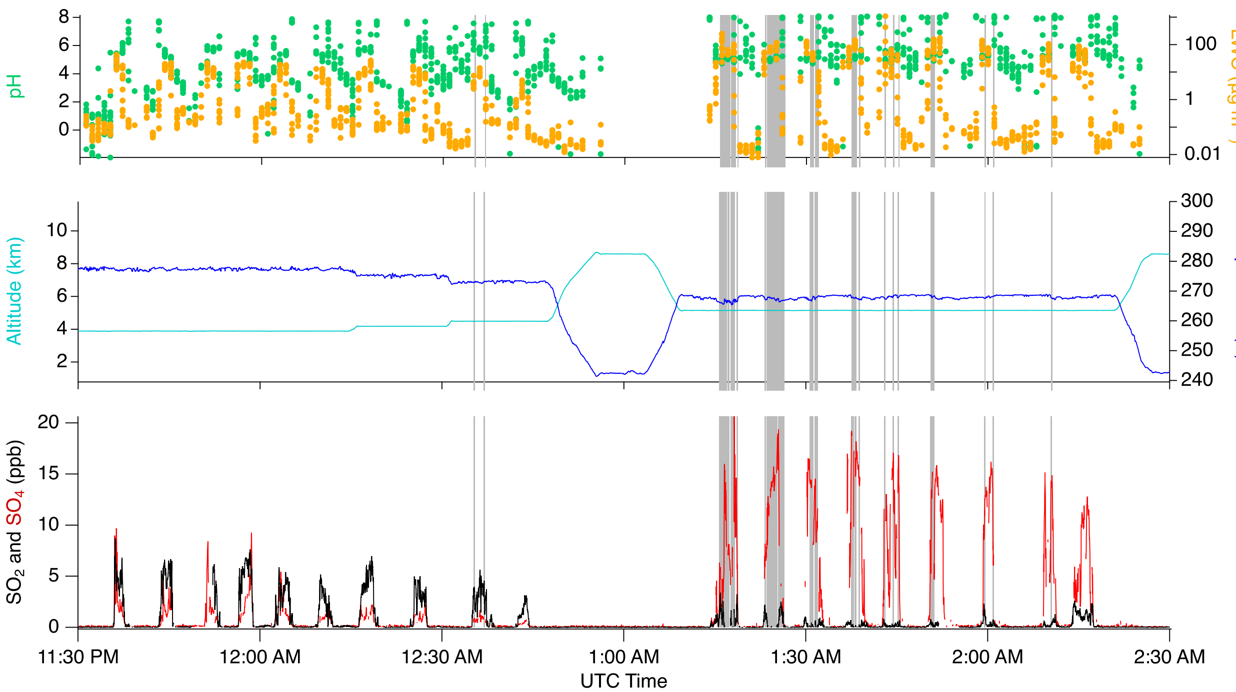

Figure S5. Measurements of SO_2, sulfate, temperature, and altitude with calculations of pH and LWC during the 7 August 2019 flight.

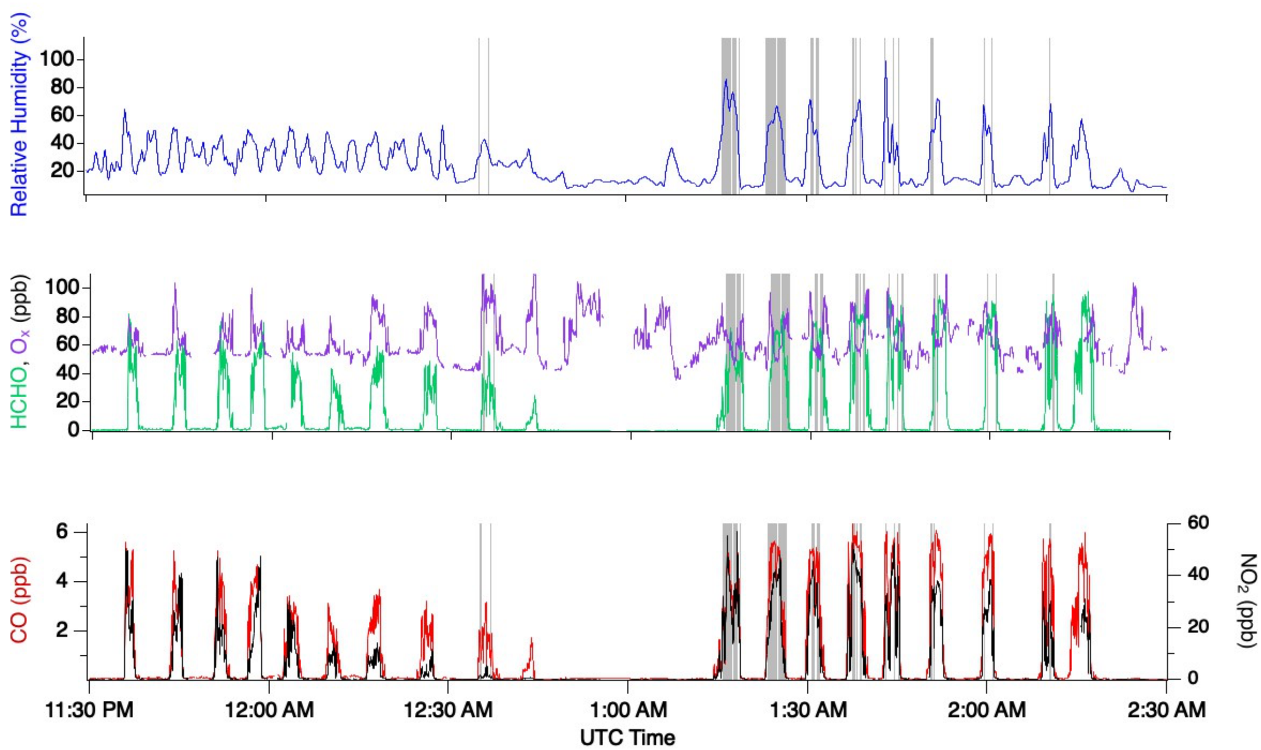

Figure S6. Measurements of relative humidity, HCHO, O_x ($O_3 + NO_2$), SO_2, and CO during the 7 August 2019 flight with clouds indicated by the grey bars.

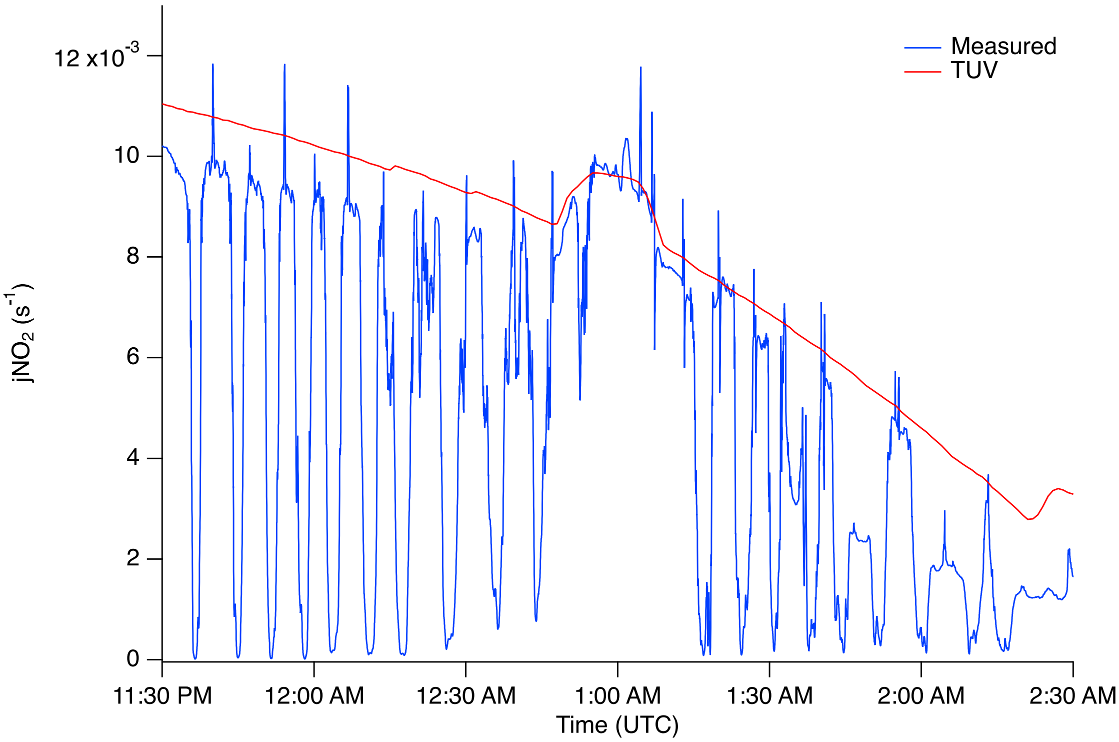

Figure S7. Actinic flux measurements of jNO_2 (blue) during the 7 August flight for both passes compared to clear-sky reference calculations from the Tropospheric Ultraviolet and Visible (TUV) radiative transfer model (Madronich and Flocke, 1999) (red).

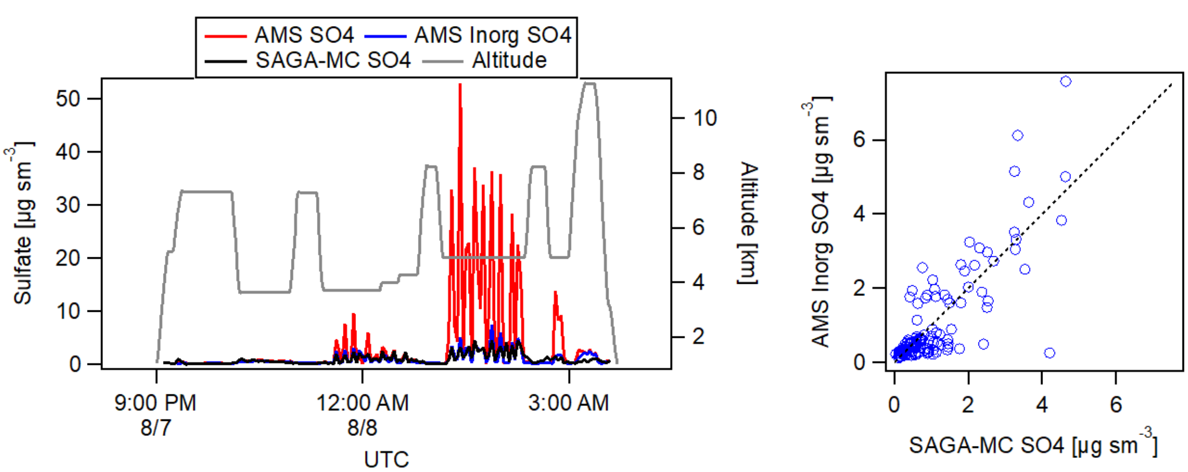

Figure S8. Comparison of organic sulfur to inorganic sulfate as measured during the FIREX-AQ 7 August flight (left) and correlation of AMS apportioned inorganic sulfate to SAGA mist chamber measurements (right).

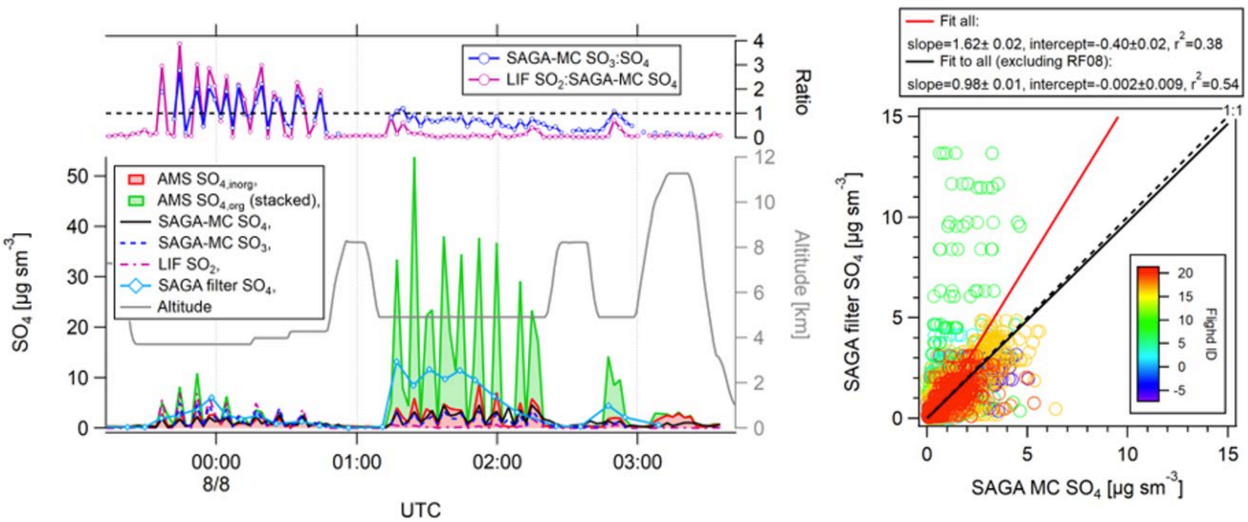

Figure S9. Comparison of AMS inorganic and organic sulfate concentrations, SAGA MC sulfate and S(IV) (reported as SO_3), and LIF SO_2 between the two passes (left) and correlation of SAGA filter sulfate to SAGA MC sulfate (right).

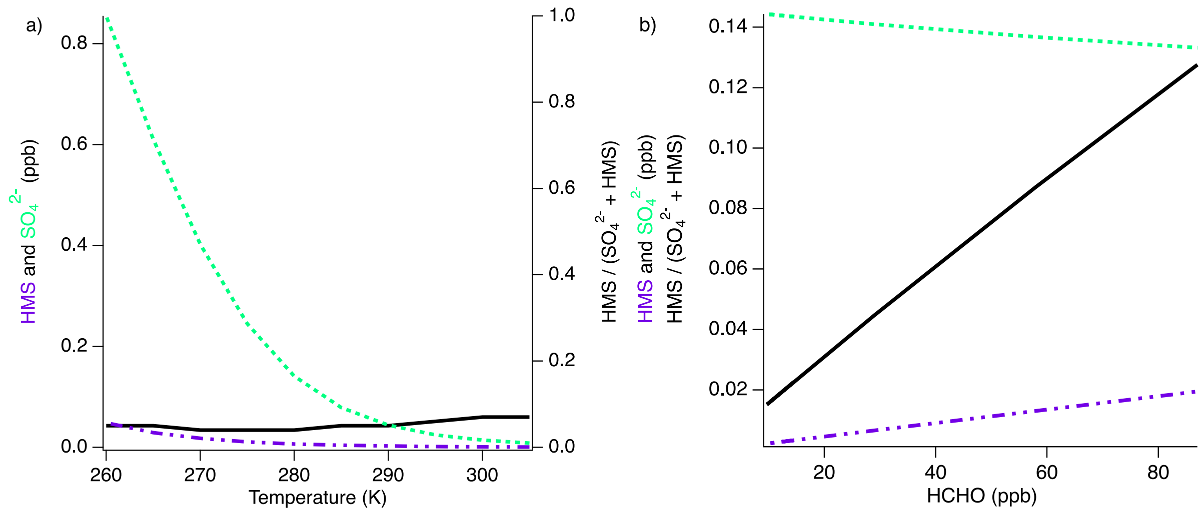

Figure S10. Model HMS and sulfate production with varied temperature (a) and HCHO (b) under the conditions of the 3 August 2019 flight.

Section 2: Sulfur conversion mechanism

The sulfure conversion mechanism code describes the process of converting SO_2 to sulfate and HMS based on the rate constants included in Table S1. This code is meant to be used in Matlab with F0AM (https://github.com/AirChem/F0AM (doi.org/10.5281/zenodo.5752566)).

```
SpeciesToAdd = {'SO2','SO2aq','HSO3_','SO3_2','O3','O3aq','H2O2','H2O2aq','Haq','SO4_2','H2Oaq',...
    'OH_','O2aq','SO4','NO2','NO2_','NO2aq', 'HCHO', 'HCHOaq', 'CH2OHSO3_','O2aq','H2SO4'};

AddSpecies

%%%%% Sulfur equilibrium reactions

i=i+1;
Rnames{i} = 'SO2 = SO2aq';
k(:,i) = khet_SO2;
Gstr{i,1} = 'SO2';
fSO2(i)=fSO2(i)-1; fSO2aq(i)=fSO2aq(i)+1;

i=i+1;
Rnames{i} = 'SO2 = HSO3_ + Haq';
k(:,i) = khet_SO2;
Gstr{i,1} = 'SO2';
fSO2(i)=fSO2(i)-1; fHSO3_(i)=fHSO3_(i)+1; fHaq(i)=fHaq(i)+1;

i=i+1;
Rnames{i} = 'SO2 = SO3_2 + Haq + Haq';
k(:,i) = khet_SO2;
Gstr{i,1} = 'SO2';
fSO2(i)=fSO2(i)-1; fSO3_2(i)=fSO3_2(i)+1; fHaq(i)=fHaq(i)+1; fHaq(i)=fHaq(i)+1;

i=i+1;
Rnames{i} = 'SO2aq = SO2';
k(:,i) = khet_SO2./H_SO2.*M./P./6.022E20./lwc;
Gstr{i,1} = 'SO2aq';
fSO2aq(i)=fSO2aq(i)-1; fSO2(i)=fSO2(i)+1;

i=i+1;
Rnames{i} = 'HSO3_ = SO2';
```

```
k(:,i) = khet_SO2./H_SO2.*M./P./6.022E20./HSO3./lwc;
Gstr{i,1} = 'HSO3_';
fHSO3_(i)=fHSO3_(i)-1; fSO2(i)=fSO2(i)+1;

i=i+1;
Rnames{i} = 'SO3_2 = SO2';
k(:,i) = khet_SO2./H_SO2.*M./P./6.022E20./SO3_2./lwc;
Gstr{i,1} = 'SO3_2';
fSO3_2(i)=fSO3_2(i)-1; fSO2(i)=fSO2(i)+1;

%%%%% Oxidation reactions

i=i+1;
Rnames{i} = 'O3 = O3aq';
k(:,i) = khet_O3 ;
Gstr{i,1} = 'O3';
fO3(i)=fO3(i)-1; fO3aq(i)=fO3aq(i)+1;

i=i+1;
Rnames{i} = 'O3aq = O3';
k(:,i) = khet_O3./H_O3.*M./P./6.022E20./lwc;
Gstr{i,1} = 'O3aq';
fO3aq(i)=fO3aq(i)-1; fO3(i)=fO3(i)+1;

i=i+1;
Rnames{i} = 'O3aq + SO2aq = H2SO4 + O2aq';
k(:,i) = 2.4E4./6.022E20./lwc ;
Gstr{i,1} = 'O3aq'; Gstr{i,2} = 'SO2aq';
fO3aq(i)=fO3aq(i)-1; fSO2aq(i)=fSO2aq(i)-1; fO2aq(i)=fO2aq(i)+1;  fH2SO4(i)=fH2SO4(i)+1;

i=i+1;
Rnames{i} = 'O3aq + HSO3_ = SO4_2 + Haq + O2aq';
k(:,i) = O3_ox1./6.022E20./lwc ;
Gstr{i,1} = 'O3aq'; Gstr{i,2} = 'HSO3_';
fO3aq(i)=fO3aq(i)-1; fHSO3_(i)=fHSO3_(i)-1; fSO4_2(i)=fSO4_2(i)+1;  fHaq(i)=fHaq(i)+1;  fO2aq(i)=fO2aq(i)+1;

i=i+1;
Rnames{i} = 'O3aq + SO3_2 = SO4_2 + O2aq';
k(:,i) = O3_ox2./6.022E20./lwc ;
Gstr{i,1} = 'O3aq'; Gstr{i,2} = 'SO3_2';
```

```
fO3aq(i)=fO3aq(i)-1; fSO3_2(i)=fSO3_2(i)-1; fSO4_2(i)=fSO4_2(i)+1;  fO2aq(i)=fO2aq(i)+1;


i=i+1;
Rnames{i} = 'H2O2 = H2O2aq';
k(:,i) = khet_H2O2 ;
Gstr{i,1} = 'H2O2';
fH2O2(i)=fH2O2(i)-1; fH2O2aq(i)=fH2O2aq(i)+1;

i=i+1;
Rnames{i} = 'H2O2aq = H2O2';
k(:,i) = khet_H2O2./H_H2O2.*M./P./6.022E20./lwc;
Gstr{i,1} = 'H2O2aq';
fH2O2aq(i)=fH2O2aq(i)-1; fH2O2(i)=fH2O2(i)+1;

i=i+1;
Rnames{i} = 'H2O2aq + HSO3_ = SO4_2 + Haq + Haq + H2Oaq';
k(:,i) = H2O2aq_ox./6.022E20./lwc ;
Gstr{i,1} = 'H2O2aq'; Gstr{i,2} = 'HSO3_';
fH2O2aq(i)=fH2O2aq(i)-1; fHSO3_(i)=fHSO3_(i)-1; fSO4_2(i)=fSO4_2(i)+1;  fHaq(i)=fHaq(i)+1;  fHaq(i)=fHaq(i)+1;  fH2Oaq(i)=fH2Oaq(i)+1;

i=i+1;
Rnames{i} = 'NO2 = NO2aq';
k(:,i) = khet_NO2 ;
Gstr{i,1} = 'NO2';
fNO2(i)=fNO2(i)-1; fNO2aq(i)=fNO2aq(i)+1;

i=i+1;
Rnames{i} = 'NO2aq = NO2';
k(:,i) = khet_NO2./H_NO2.*M./P./6.022E20./lwc;
Gstr{i,1} = 'NO2aq';
fNO2aq(i)=fNO2aq(i)-1; fNO2(i)=fNO2(i)+1;

i=i+1;
Rnames{i} = 'NO2aq + NO2aq + HSO3_ = Haq + Haq + Haq + NO2_ + NO2_ + SO4_2';
k(:,i) = 1E6./6.022E20./lwc;
Gstr{i,1} = 'NO2aq'; Gstr{i,2} = 'HSO3_'; Gstr{i,3} = 'NO2aq';
fNO2aq(i)=fNO2aq(i)-1; fNO2aq(i)=fNO2aq(i)-1; fHSO3_(i)=fHSO3_(i)-1; fNO2_(i)=fNO2_(i)+1; fNO2_(i)=fNO2_(i)+1; fSO4_2(i)=fSO4_2(i)+1;

i=i+1;
```

```
Rnames{i} = 'NO2aq + NO2aq + SO3_2 = H2O + NO2_ + NO2_ + SO4_2';
k(:,i) = 1.4E10./6.022E20./lwc;
Gstr{i,1} = 'NO2aq'; Gstr{i,2} = 'SO3_2'; Gstr{i,3} = 'NO2aq';
fNO2aq(i)=fNO2aq(i)-1; fNO2aq(i)=fNO2aq(i)-1; fSO3_2(i)=fSO3_2(i)-1; fNO2_(i)=fNO2_(i)+1; fNO2_(i)=fNO2_(i)+1; fSO4_2(i)=fSO4_2(i)+1;

i=i+1;
Rnames{i} = 'HCHO = HCHOaq';
k(:,i) = khet_HCHO;
Gstr{i,1} = 'HCHO';
fHCHO(i)=fHCHO(i)-1; fHCHOaq(i)=fHCHOaq(i)+1;

i=i+1;
Rnames{i} = 'HCHOaq = HCHO';
k(:,i) = khet_HCHO./H_HCHO.*M./P./6.022E20./lwc;
Gstr{i,1} = 'HCHOaq';
fHCHOaq(i)=fHCHOaq(i)-1; fHCHO(i)=fHCHO(i)+1;

i=i+1;
Rnames{i} = 'HCHOaq + HSO3_ = CH2OHSO3_';
k(:,i) = 7.9E2.*exp(-4900.*(1./T-1./298))./6.022E20./lwc ;
Gstr{i,1} = 'HCHOaq'; Gstr{i,2} = 'HSO3_';
fHCHOaq(i)=fHCHOaq(i)-1; fHSO3_(i)=fHSO3_(i)-1; fCH2OHSO3_(i)=fCH2OHSO3_(i)+1;

i=i+1;
Rnames{i} = 'HCHOaq + SO3_2 = CH2OHSO3_ + OH_';
k(:,i) = 2.5E7.*exp(-1800.*(1./T-1./298))./6.022E20./lwc ;
Gstr{i,1} = 'HCHOaq'; Gstr{i,2} = 'SO3_2';
fHCHOaq(i)=fHCHOaq(i)-1; fSO3_2(i)=fSO3_2(i)-1; fCH2OHSO3_(i)=fCH2OHSO3_(i)+1; fOH_(i)=fOH_(i)+1;

i=i+1;
Rnames{i} = 'CH2OHSO3_ = HCHOaq + SO3_2';
k(:,i) = (6.2E-8.*exp(-11400.*(1./T-1./298))+4.8E3.*(Kw./Haq).*exp(-4700.*(1./T-1./298)))./2 ;
Gstr{i,1} = 'CH2OHSO3_';
fCH2OHSO3_(i)=fCH2OHSO3_(i)-1; fHCHOaq(i)=fHCHOaq(i)+1; fSO3_2(i)=fSO3_2(i)+1;

i=i+1;
Rnames{i} = 'CH2OHSO3_ = HCHOaq + HSO3_';
k(:,i) = (6.2E-8.*exp(-11400.*(1./T-1./298))+4.8E3.*(Kw./Haq).*exp(-4700.*(1./T-1./298)))./2 ;
Gstr{i,1} = 'CH2OHSO3_';
fCH2OHSO3_(i)=fCH2OHSO3_(i)-1; fHCHOaq(i)=fHCHOaq(i)+1; fHSO3_(i)=fHSO3_(i)+1;
```

References

Boniface, J., Shi, Q., Li, Y. Q., Cheung, J. L., Rattigan, O. V., Davidovits, P., Worsnop, D. R., Jayne, J. T., and Kolb, C. E.: Uptake of Gas-Phase SO2, H2S, and CO2 by Aqueous Solutions, J. Phys. Chem. A 2000, 104, 32, 7502–7510, https://doi.org/10.1021/jp000479h, 2000.

Boyce, S. D. and Hoffman, M. R.: Kinetics and mechanism of the formation of hydroxymethanesulfonic acid at low pH, J. Phys. Chem. 88, 4740-4746, https://doi.org/10.1021/j150664a059, 1984.

Cheng, A., Zheng, G., Wei, C., Mu, Q., Zheng, B., Wang, Z., Gao, M., Zhang, Q., He, K., Carmichael, G., Pöschl, U., and Su, H.: Reactive nitrogen chemistry in aerosol water as a source of sulfate during haze events in China, Sci. Adv., 2(12) 1-11, DOI: 10.1126/sciadv.1601530, 2016.

D'Ambro, E. L., Moller, K. H., Lopez-Hilfiker, F. D., Schobesberger, S., Liu, J., Shilling, J. E., Lee, B. H., Kjaergaard, H. G., and Thornton, J. A.: Isomerization of Second-Generation Isoprene Peroxy Radicals: Epoxide Formation and Implications for Secondary Organic Aerosol Yields, Environ. Sci. Technol., 51(9), 4978-4987, https://doi.org/10.1021/acs.est.7b00460, 2016.

Deister, U., Neeb, R., Helas, G., and Warneck, P.: Temperature dependence of the equilibrium CH2(OH)2 + HSO3- = CH2(OH)SO3- + H2O in aqueous solution, J. Phys. Chem., 90, 3213-3217, 10.1021/j100405a033, 1986.

Ding, J., Zhao, P., Su, J., Dong, Q., Du, X., and Zhang, Y.: Aerosol pH and its driving factors in Beijing, Atmos. Chem. Phys., 19, 7939–7954, https://doi.org/10.5194/acp-19-7939-2019, 2019.

Dovrou, E., Lim, C. Y., Canagaratna, M. R., Kroll, J. H., Worsnop, D. R., and Keutsch, F. N.: Measurement techniques for identifying and quantifying hydroxymethanesulfonate (HMS) in an aqueous matrix and particulate matter using aerosol mass spectrometry and ion chromatography, Atmos. Meas. Tech., 12, 5303–5315, https://doi.org/10.5194/amt-12-5303-2019, 2019.

Finlayson-Pitts B.J. and Pitts J.N., Jr.: Chemistry of the Upper and Lower Atmosphere: Theory, Experiments, and Applications (Academic, San Diego), 1999.

George, C., Pnoche, J. L., and Mirabel, P.: Experimental Determination of Mass Accommodation Coefficient, Nucleation and Atmospheric Aerosols, A. Deepak Publishing, Hampton, VA, 1992.

Guo, H., Xu, L., Bougiatioti, A., Cerully, K. M., Capps, S. L., Hite Jr., J. R., Carlton, A. G., Lee, S.-H., Bergin, M. H., Ng, N. L., Nenes, A., and Weber, R. J.: Fine-particle water and pH in the southeastern United States, Atmos. Chem. Phys., 15, 5211–5228, https://doi.org/10.5194/acp-15-5211-2015, 2015.

Guo, H., Weber, R. J., and Nenes, A.: High levels of ammonia do not raise fine particle pH sufficiently to yield nitrogen oxide-dominated sulfate production, Scientific Reports, 7(1), https://doi.org/10.1038/s41598-017-11704-0, 2017.

Hennigan, C. J., Izumi, J., Sullivan, A. P., Weber, R. J., and Nenes, A.: A critical evaluation of proxy methods used to estimate the acidity of atmospheric particles, Atmos. Chem. Phys., 15, 2775–2790, https://doi.org/10.5194/acp-15-2775-2015, 2015.

Heyerdahl, E. K., Brubaker, L. B., and Agee, J. K.: Annual and decadal climate forcing of historical fire regimes in the interior Pacific Northwest, USA, The Holocene, 12(5), 597-604, https://doi.org/10.1191/0959683602hl570rp, 2002.

Hoffmann, M. R., and J. G. Calvert, Chemical transportation modules for Eulerian acid deposition models, vol. II, The aqueous-phase chemistry, Rep. EPA/600/3-85/017, Environ. Prot. Agency, Research Triangle Park, N. C., 1985.

Kok, G. L., Gitlin, S. N., and Lazrus, A. L.: Kinetics of the formation and decomposition of hydroxymethanesulfonate, J. Geophys. Res. Atmos., 91, 2801-2804, 10.1029/JD091iD02p02801, 1986.

Kreidenweis, S. M., C. J. Walcek, G. Feingold, W. Gong, M. Z. Jacobson, C.-H. Kim, X. Liu, J. E. Penner, A. Nenes, and J. H. Seinfeld, Modification of aerosol mass and size distribution due to aqueous-phase SO2 oxidation in clouds: Comparisons of several models, J. Geophys. Res., 108(D7), 4213, doi:10.1029/2002JD002697, 2003.

Liu, T. and Abbatt, J. P. D.: Oxidation of sulfur dioxide by nitrogen dioxide accelerated at the interface of deliquesced aerosol particles, Nat. Chem., 13, 1173-1177, https://doi.org/10.1038/s41557-021-00777-0, 2021.

Madronich, S. and Flocke, S.: The Role of Solar Radiation in Atmospheric Chemistry, in: Environmental Photochemistry, The Handbook of Environmental Chemistry (Reactions and Processes), edited by: Boule, P., vol. 2/2L, Springer, Berlin, Heidelberg, 1999.

Moch, J. M., Dovrou, E., Mickley, L. J., Keutsch, F. N., Cheng, Y., Jacob, D. J., Jiang, J., Li M., Munger, J. W., Qiao, X., and Zhang, Q.: Contribution of hydroxymethane sulfonate to ambient particulate matter: A potential explanation for high particulate sulfur during severe winter haze in Beijing, Geophys. Res. Lett., 45, 11,969-11,979, https://doi.org/10.1029/2018GL079309, 2018.

Olson, T. M. and Fessenden, R. W.: Pulse radiolysis study of the reaction of hydroxyl radicals with methanesulfonate and hydroxymethanesulfonate, J. Phys. Chem., 96(8), 3317-3320, https://doi.org/10.1021/j100187a027, 1992.

Pye, H. O. T., Nenes, A., Alexander, B., Ault, A. P., Barth, M. C., Clegg, S. L., Collett, J. L., Jr., Fahey, K. M., Hennigan, C. J., Herrmann, H., Kanakidou, M., Kelly, J. T., Ku, I.-T., McNeill, V. F., Riemer, N., Schaefer, T., Shi, G., Tilgner, A., Walker, J. T., Wang, T., Weber, R., Xing, J., Zaveri, R. A., and Zuend, A.: The acidity of atmospheric particles and clouds, Atmos. Chem. Phys., 20, 4809–4888, 2020.

Seinfeld, J. H., and Pandis, S. N.: Atmospheric Chemistry and Physics: From Air Pollution and Climate Change, John Wiley, New York, 2006.

Shao, J., Chen, Q., Wang, Y., Lu, X., He, P., Sun, Y., Shah, V., Martin, R. V., Philip, S., Song, S., Zhao, Y., Xie, Z., Zhang, L., and Alexander, B.: Heterogeneous sulfate aerosol formation mechanisms during wintertime Chinese haze events: air quality model assessment using observations of sulfate oxygen isotopes in Beijing, Atmos. Chem. Phys., 19, 6107–6123, https://doi.org/10.5194/acp-19-6107-2019, 2019.

Song, S., Gao, M., Xu, W., Sun, Y., Worsnop, D. R., Jayne, J. T., Zhang, Y., Zhu, L., Li, M., Zhou, Z., Cheng, C., Lv, Y., Wang, Y., Peng, W., Xu, X., Lin, N., Wang, Y., Wang, S., Munger, J. W., Jacob, D. J., and McElroy, M. B.: Possible heterogeneous chemistry of hydroxymethanesulfonate (HMS) in northern China winter haze, Atmos. Chem. Phys., 19, 1357–1371, https://doi.org/10.5194/acp-19-1357-2019, 2019.

Song, S., Ma, T., Zhang, Y., Shen, L., Liu, P., Li, K., Zhai, S., Zheng, H., Gao, M., Moch, J. M., Duan, F., He, K., and McElroy, M. B.: Global modeling of heterogeneous hydroxymethanesulfonate chemistry, Atmos. Chem. Phys., 21, 457–481, https://doi.org/10.5194/acp-21-457-2021, 2021.

Tang, M. J., Telford, P. J., Pope, F. D., Rkiouak, L., Abraham, N. L., Archibald, A. T., Braesicke, P., Pyle, J. A., McGregor, J., Watson, I. M., Cox, R. A., and Kalberer, M.: Heterogeneous reaction of N2O5 with airborne TiO2 particles and its implication for stratospheric particle injection, Atmos. Chem. Phys., 14, 6035–6048, https://doi.org/10.5194/acp-14-6035-2014, 2014.

Toda, K., Yunoki, S., Yanaga, A., Takeuchi, M., Ohira, S.-I., and Dasgupta, P. K.: Formaldehyde Content of Atmospheric Aerosol, Environ. Sci. Technol. 2014, 48, 12, 6636–6643, https://doi.org/10.1021/es500590e, 2014.

Vieceli, J., Roeselová, M., Potter, N., Dang, L. X., Garret, B. C., and Tobias, D. J.: Molecular Dynamics Simulations of Atmospheric Oxidants at the Air−Water Interface: Solvation and Accommodation of OH and O3, J. Phys. Chem. B 2005, 109, 33, 15876–15892, https://doi.org/10.1021/jp051361, 2005.

Ye, C., Chen, H., Hoffmann, E. H., Mettke, P., Tilgner, A., He, L., Mutzel, A., Brüggemann, M., Poulain, L., Schaefer, T., Heinold, B., Ma, Z., Liu, P., Xue, C., Zhao, X., Zhang, C., Zhang, F., Sun, H., Li, Q., Wang, L., Yang, X., Wang, J., Liu, C., Xing, C., Mu, Y., Chen, J., and Herrmann, H.: Particle-Phase Photoreactions of HULIS and TMIs Establish a Strong Source of H2O2 and Particulate Sulfate in the Winter North China Plain, Environ. Sci. Technol., https://doi.org/10.1021/acs.est.1c00561, 2021.

Zhang, R., Wang, G., Guo, S., Zamora, M. L., Ying, Q., Lin, Y., Wang, W., Hu, M., Wang, Y.: Formation of urban fine particulate matter. Chem. Rev., 115, 3803−3855, https://doi.org/10.1021/acs.chemrev.5b00067, 2015.